JACC: CARDIOVASCULAR IMAGING
VOL. 8, NO. 12, 2015
© 2015 BY THE AMERICAN COLLEGE OF CARDIOLOGY FOUNDATION
ISSN 1936-878X/$36.00
PUBLISHED BY ELSEVIER
http://dx.doi.org/10.1016/j.jcmg.2015.11.001

Tissue Tracking Technology for Assessing Cardiac Mechanics

Principles, Normal Values, and Clinical Applications

Piet Claus, PhD,* Alaa Mabrouk Salem Omar, MD, PhD,†‡ Gianni Pedrizzetti, PhD,§ Partho P. Sengupta, MD, DM,† Eike Nagel, MD, PhD‖

ABSTRACT

Tissue tracking technologies such as speckle tracking echocardiography and feature tracking cardiac magnetic resonance have enhanced the noninvasive assessment of myocardial deformation in clinical research and clinical practice. The widespread enthusiasm for using tissue tracking techniques in research and clinical practice stems from the ready applicability of these technologies to routine echocardiographic or cardiac magnetic resonance images. The technology is common to both modalities, and derived parameters to describe myocardial mechanics are the similar, albeit with different accuracies. We provide an overview of the normal values and reproducibility of the clinically applicable parameters, together with their clinical validation. The use of these technologies in different clinical scenarios, and the additive value to current imaging diagnostics are discussed. (J Am Coll Cardiol Img 2015;8:1444–60) © 2015 by the American College of Cardiology Foundation.

Optimal management of patients with cardiovascular disease is increasingly based on algorithms that use cutoff values or continuous variables, rather than simple binary ("yes" or "no") decision trees. Accordingly, cardiac imaging techniques such as echocardiography and cardiac magnetic resonance (CMR) imaging have been developed for providing diagnostic information that are often expressed numerically. Both techniques can measure cardiac muscle motion and deformation; however, more recently, the clinical focus for noninvasive deformation imaging is moving from tailored acquisitions, such as tissue Doppler imaging or myocardial tagging, to post-processing of standard grayscale B-mode or cine imaging, resulting in easier access and wider availability. This review focuses on the current status of these post-processing methods, commonly known as tissue tracking, irrespective of the imaging modality. Speckle tracking echocardiography (2-dimensional [2D] and 3-dimensional [3D]) and feature tracking in CMR are compared and contrasted for elucidating relative strength and pitfalls and solutions that address modality-related differences.

TECHNOLOGY OF TISSUE TRACKING

As shown in the **Central Illustration**, the technology of tissue tracking refers to methods of identifying a peculiar pattern along a curve on 1 image, such as the endocardial border, and recognizing the same pattern within a second image taken a few instants later. In this way, displacement of myocardial segments can be estimated. In echocardiography, images are characterized by the presence of speckles with a certain persistence (1,2); thus, the technique is commonly referred to as speckle tracking echocardiography (STE) both in 2 and 3 dimensions; in CMR, where tissue

From the *Laboratory for Cardiovascular Imaging and Dynamics, Department of Cardiovascular Sciences, KU Leuven, Leuven, Belgium; †Zena and Michael A. Wiener Cardiovascular Institute, Icahn School of Medicine at Mount Sinai, New York, New York; ‡Department of Internal Medicine, Medical Division, National Research Centre, Dokki, Cairo, Egypt; §Department of Engineering and Architecture, University of Trieste, Trieste, Italy; and the ‖Institute of Cardiovascular Imaging, Goethe University Frankfurt and German Centre for Cardiovascular Research ([DZHK], partner site Rhine-Main), Frankfurt, Germany.
Dr. Claus receives financial support from KU Leuven under grant #PF/10/014. Dr. Omar is a consultant/advisor for Edwards Lifesciences. Dr. Pedrizzetti receives financial support from the Italian government (grant #PRIN N. 2012HMR7CF_002) and is a shareholder of AMID. Dr. Sengupta is a consultant/advisor for Edwards Lifesciences, Saffron Technology, Heart Test Labs, and TeleHealthRobotics; and receives research support from Forest Laboratories. Dr. Nagel receives support in kind (analysis software) from TomTec Imaging Systems, and from Circle Cardiovascular Imaging Inc. Drs. Claus and Omar contributed equally to this paper.

Manuscript received October 28, 2015; accepted November 6, 2015.

regions are identified by individual anatomical features, they are usually referred to as feature tracking (FT) (3).Thus, the intrinsic differences in both techniques are related to what region of myocardium is tracked, which may lead to differences in measurements.

All tracking techniques are more robust and reproducible for global rather than regional values. Dependent on image quality, 2D-STE is making it difficult in instances of poor echogenic windows, ultrasound dropouts, and reverberations. Through-plane motion may limit measurements in 2D-STE due to difficulties in tracking speckles that fall out of plane in subsequent tracking frames. In the distal part of the ultrasound sector, image quality deteriorates, resulting in a better tracking quality of speckles that are located proximally (4).

The problem of through-plane motion can be solved by using 3D echocardiographic techniques (i.e., 3D-STE) that recently became possible with advancements in matrix-array ultrasound transducers. In principle, the same tracking technology can be applied to 3D volumetric regions without conceptual differences, resulting in the availability of several 3D tissue tracking solutions. Unlike 2D-STE, speckles can be tracked simultaneously in all directions to derive all deformation parameters, alleviating the effect of through-plane motion and allowing for assessment of speckles independent from specific imaging planes. However, 3D images present a substantially (at least 3× to 4×) lower spatial as well as lower temporal resolution than their 2D counterpart does. This limitation in combination with the remaining dependency of the data on image quality so far makes 3D-STE assessments still controversial and their true value remains unknown (5). Further technical developments are required for improving 3D-STE accuracy.

FT-CMR has been explored on stacks of 2D cine images, with a typical slice distance of 6 to 8 mm and strong contrast between blood pool and myocardium, but with a lower in-plane spatial (1 to 2 mm) and temporal resolution (commonly 30 phases per heart cycle) than with 2D-STE. FT-CMR on 2D stacks suffers also from through-plane motion effects. Temporal averaging may result in lower strain values for FT-CMR in comparison to STE. Due to the lack of intramyocardial features, FT-CMR algorithms focus on the endocardial and epicardial borders with a stronger weighing of endocardial deformation explaining some of the differences in results found in direct comparisons of FT-CMR and STE. From the displacement estimations provided by these tracking methodologies a series of deformation parameters relevant to assess the mechanics of the myocardium can be derived (**Table 1**).

NORMAL VALUES, REPRODUCIBILITY, AND CLINICAL VALIDATION

Tissue tracking can be used in the assessment of the mechanics of all cardiac chambers. Whereas the assessment of left ventricular (LV) and right ventricular (RV) deformations are of established clinical benefit, tissue tracking has been also used in studies to assess atrial deformations, mostly of the left atrium (LA); however, clinical applications remain to be validated.

SPECKLE TRACKING ECHOCARDIOGRAPHY. Global longitudinal strain (GLS) averaged from the apical views is the most robust and reproducible of all LV deformation parameters and has been shown to be a powerful diagnostic and prognostic tool. The use of LV- and RV-GLS is recommended in most recent guidelines for the quantitative assessment of LV and RV function (6). Due to a wide range of normal cutoff values (−17.3% to −21.5%) when measured by different vendors (6), guidelines are not recommending a clear cutoff value for LV-GLS but suggest that peak systolic LV-GLS in a healthy individual should be approximately -20%. Lower values should be expected in male patients and with increasing age and heart rate, as well as loading conditions, will influence the results (6,7). Serial measurements in an individual patient should be carried out using the same vendor machine and software (6).

RV-GLS and strain rate can be derived from tracking the RV free wall and the LV septum or only from the RV free wall in a RV focused apical 4-chamber view; however, RV free wall measurements were found to be of more prognostic value (6). Pooled data from single-center studies suggest that normal RV-GLS derived from the free wall should be lower than -20% (6).

It is important to note that GLS has better reproducibility than other LV deformation indices. Normal values of global circumferential strain (GCS) range between −20.9% and −27.8%, and global radial strain (GRS) between 35.1% and 59.0%, with mean values of −23.3% and 47.3%, respectively (8). The assessment of LV rotational mechanics suffers additionally from the lack of a standardized method of LV apical short-axis acquisition. Only small studies defining

ABBREVIATIONS AND ACRONYMS

2D = 2-dimensional
3D = 3-dimensional
ARVC = arrhythmogenic right ventricular cardiomyopathy
AS = aortic stenosis
CAD = coronary artery disease
CMR = cardiac magnetic resonance
CP = constrictive pericarditis
CRT = cardiac resynchronization therapy
DCM = dilated cardiomyopathy
EF = ejection fraction
FT = feature tracking
GCS = global circumferential strain
GLS = global longitudinal strain
GRS = global radial strain
HCM = hypertrophic cardiomyopathy
HFpEF = heart failure with preserved ejection fraction
HFrEF = heart failure with reduced ejection fraction
LA = left atrium
LS = longitudinal strain
LV = left ventricle
LVT = left ventricular twist
MR = mitral regurgitation
PAH = primary arterial hypertension
RCM = restrictive cardiomyopathy
RV = right ventricle
STE = speckle tracking echocardiography

CENTRAL ILLUSTRATION **Current Tissue Tracking Technology to Assess Early Myocardial Dysfunction**

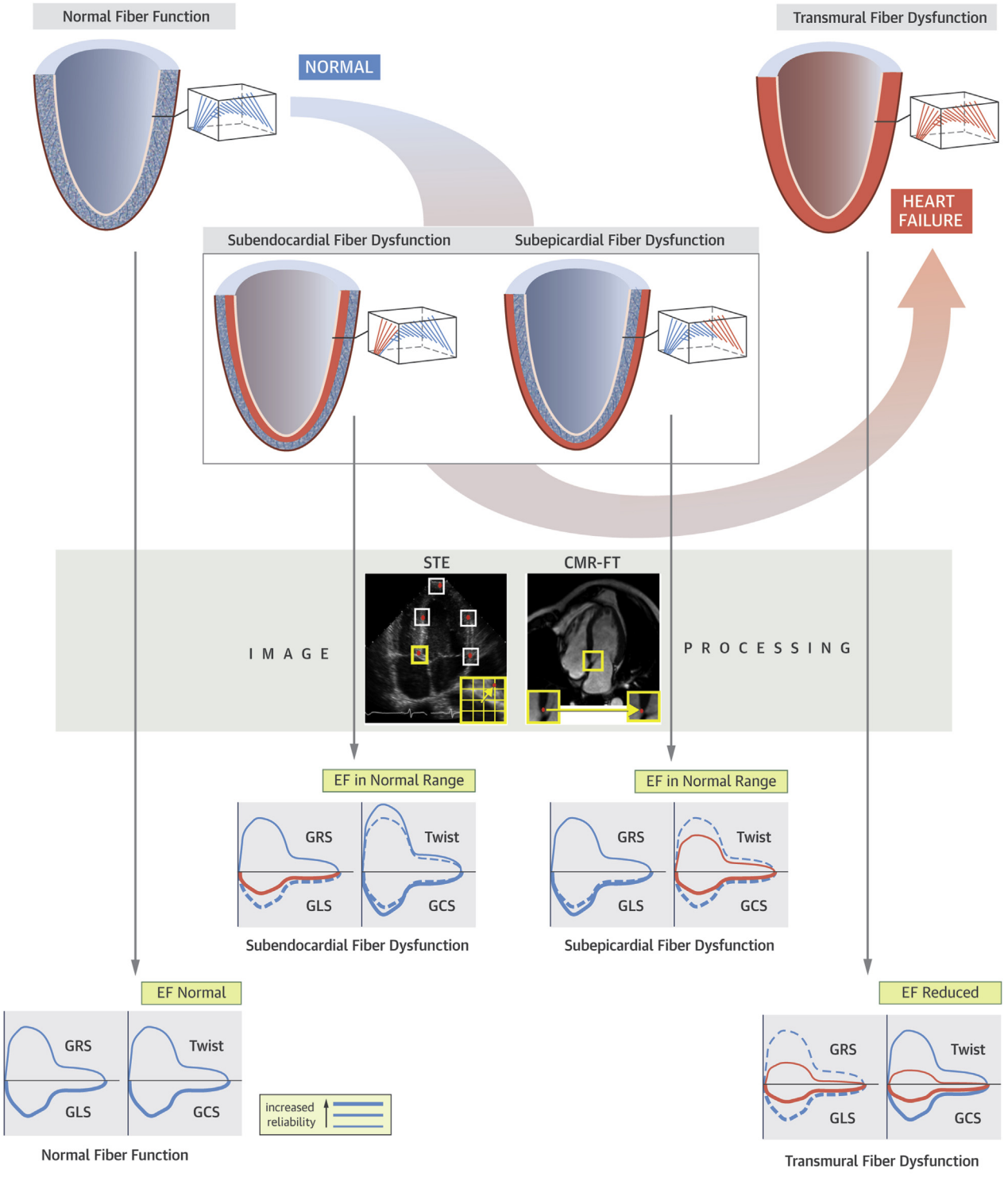

Claus, P. et al. J Am Coll Cardiol Img. 2015; 8(12):1444–60.

Continued on the next page

TABLE 1 Main Clinically Applicable Cardiac Mechanics Variables Derived From Tracking Technology

	Definition	Parameters
Displacement, cm	Distance between instantaneous and initial (often end-diastolic) position of a myocardial segment	Longitudinal displacement Radial displacement Circumferential displacement
Velocity, cm/s	Velocity of displacement (displacement/time) accuracy is highly frame-rate dependent	Longitudinal velocity Radial velocity Circumferential velocity
Strain, %	Change in length of an object within a certain direction relative to its initial (often end-diastolic) length	Global/segmental longitudinal strain (GLS/LS) Global/segmental radial strain (GRS/RS) Global/segmental circumferential strain (GCS/CS)
Strain rate, 1/s	The speed of deformation accuracy is highly frame-rate dependent	Peak systolic global longitudinal strain rate (GLSR-S) Early diastolic global longitudinal strain rate (GLSR-E) Late diastolic global longitudinal strain rate (GLSR-A) Peak systolic global radial strain rate (GRSR-S) Early diastolic global radial strain rate (GRSR-E) Late diastolic global radial strain rate (GRSR-A) Peak systolic global circumferential strain rate (GCSR-S) Early diastolic global circumferential strain rate (GCSR-E) Late diastolic global circumferential strain rate (GCSR-A)
Rotation	Results from shortening and lengthening of helically oriented myocardial fibers causing counterclockwise rotation of the apex and clockwise rotation of the base as viewed from the apex	Peak systolic apical rotation (apical-R) Peak systolic basal rotation (basal-R) LV twist (LVT) LV torsion (LV-tor) Percentage of LV untwist at mitral valve opening (%LV-UT-MVO) LV untwist rate (LV-UTR) Time to peak untwist (TTP-UT)

LV = left ventricular.

age-specific normal ranges of left ventricular twist (LVT) and untwist are available. Therefore, GCS, GRS, and LVT remain deformation parameters with potential clinical value awaiting further validation.

CMR FEATURE TRACKING. Comparative normal values can be found in Table 2. For this review we included data from studies that have reported more than 1 strain component.

Across normal value studies, the most consistent parameters were GCS and GLS. In contrast, variations in GRS between studies were large and radial strains measured from long-axis acquisitions were often lower than from short-axis acquisitions, possibly attributed to through-plane motion in the short-axis scans. Normal values do not depend on field strength (9) when acquired with similar acquisition parameters including similar spatial resolution. So far no systematic studies have been performed to assess sex or age differences for FT-CMR deformation parameters or dependency on imaging parameters.

RV circumferential and radial strain and strain-rate values showed overall lower values than their LV counterparts did (10). This is consistent with RV geometrical features, having thinner walls and larger radius of curvature of the free wall.

Normal values for LA-GLS can be derived during the reservoir (29 ± 5%), conduit (21 ± 6%), and atrial contraction phases (8 ± 3%) of the atrial deformation and show an increase in atrial contraction in elderly subjects consistent with physiology of normal aging (11,12).

The reproducibility studies and clinical validation are discussed in the Online Appendix and Online Tables 1 to 3.

Summary: Deriving normal values for different deformations studied by STE and FT-CMR is not easy because of variability among studies and different

CENTRAL ILLUSTRATION Continued

Tissue Tracking technologies such as speckle tracking echocardiography (STE) or more recently feature tracking cardiac magnetic resonance (FT-CMR) enhance the noninvasive assessment of myocardial mechanics of all cardiac chambers in clinical research and enter clinical practice. Whereas a plethora of parameters describing myocardial motion and deformation (e.g., velocities, strain-rates, and strain) are available, only global longitudinal strain (GLS) and global circumferential strain (GCS) have proven to be robust and reproducible in clinical practice with current implementations of these technologies and current image acquisition. Global radial strain (GRS) and twist can be assessed, but are less reproducible. Increasingly, these technologies contribute to detect early changes in myocardial mechanics in pathology (subclinical) with normal or preserved ejection fraction (EF). In the progression to heart failure, different transmural myocardial involvement (i.e., subendocardial vs. subepicardial vs. transmural involvement) of the disease will lead to different responses in global strain components. This may allow for identifying cohorts of patients with similar presentations, prognosis, and response to therapy.

TABLE 2 Overview of Normal Values for FT-CMR

First Author, Year (Ref. #)	n	GCS (SAX)	GRS (SAX)	GRS (LAX)	GLS (LV)	GLS (RV)	GCS (RV)	GRS (RV)
Augustine et al., 2013 (86)	145	21 ± 3	25 ± 6	–	19 ± 3	–	–	–
Schuster et al., 2011 (98)	10	24 ± 7	20 ± 15	15 ± 10	16 ± 10	20 ± 14	–	–
Schuster et al., 2013 (9)								
1.5-T	10	20 ± 8	25 ± 12	17 ± 10	19 ± 11	21 ± 15	–	–
3.0-T	10	19 ± 10	23 ± 11	15 ± 9	20 ± 10	22 ± 12	–	–
Morton et al., 2012 (87); average of 3 studies	10	17 ± 5	19 ± 7	18 ± 6	20 ± 5	22 ± 6	–	–
Kutty et al., 2013 (88)	20	25 ± 2	50 ± 12	–	20 ± 5	–	–	–
Kempny et al., 2012 (76)	26	24 ± 6	28 ± 11	–	21 ± 3	24 ± 4	–	–
Padiyath et al., 2013 (89)	20	25 ± 3	51 ± 12	–	20 ± 5	20 ± 4	–	–
Heermann et al., 2014 (10)	10	–	–	–	–	19 ± 6	10 ± 4	14 ± 6

Values are n or mean ± SD. Dashes indicate data are not available.

CMR = cardiac magnetic resonance; FT = feature tracking; GCS = global circumferential strain; GLS = global longitudinal strain; GRS = global radial strain; LAX = measured on long-axis slice; LV = left ventricle; RV = right ventricle; SAX = measured in short-axis slice.

users. GLS is the most robust deformation parameter for STE and is recommended in current guidelines for the assessment of LV function. Normal values around -20% for the LV and lower than -20% for the RV have been recommended for clinical practice. For FT-CMR, GCS is more reproducible than GLS with similar normal values as STE. Radial strain shows large ranges between studies and variability of segmental strains remains too high to use them as single clinical measures.

TRANSMURALITY OF DYSFUNCTION CORRESPONDS TO PATTERNS OF MYOCARDIAL DEFORMATION

Myocardial dysfunction can be classified according to the involved myocardial layer into predominantly subendocardial myocardial dysfunction, transmural myocardial dysfunction, and subepicardial dysfunction (**Central Illustration**) (13). This classification scheme corresponds to the structural and functional subunits of the LV that govern systolic and diastolic performance (13), both of which depend on the functional integrity and the synergistic coupling of the subendocardial and subepicardial fibers' layers. Using the transmurality of myocardial involvement allows identifying cohorts of patients with similar presentations, prognosis, and response to therapy.

Noninvasive imaging techniques currently do not assess myocardial fiber mechanics. However, layer-specific strain measurements are being developed and awaiting clinical validation. The differences in direction of the subendocardial and subepicardial fibers have been related to the components of myocardial deformation for defining the transmural extent of myocardial dysfunction (**Central Illustration**). Contraction of the subendocardial fibers contributes to longitudinal shortening, whereas contraction of the subepicardial fibers contributes to circumferential shortening. Both aspects contribute to radial thickening. Myocardial rotation due to shearing forces created by sliding of myocardial fibers in the longitudinal-circumferential direction is dominated by the subepicardial layer because of the larger radius of rotation (14).

Most progressive myocardial diseases predominantly cause subendocardial dysfunction in their early stages, leading to reduction in longitudinal LV mechanics (15). Because epicardial fibers remain spared, circumferential strain and twist mechanics of the LV show normal or even increased values, compensating for the longitudinal mechanical dysfunction and thus preserve stroke volume and ejection fraction (EF). Given the coronary anatomy, ischemia causes mainly subendocardial fiber dysfunction, for example, in the presence of increased LV afterload. The development of subepicardial hypertrophy attempts to compensate for the loss of longitudinal function and reduce subendocardial wall stress, which in turn leads to the increased circumferential and rotational mechanics (16). Blood pressure control in hypertensive patients has been shown to reduce circumferential strain and LVT values with concomitant regression of subepicardial hypertrophy (17).

Transmural involvement results in concomitant subendocardial and subepicardial dysfunction resulting in attenuation of myocardial mechanics in all directions (13), with impairment of LV ejection performance. An acute large transmural infarction is a classic example where simultaneous impairment of LV longitudinal and circumferential mechanics is seen, resulting in LV systolic dysfunction.

Summary: Myocardial dysfunction can be classified according to the extent of endocardial or transmural involvement. Endocardial involvement results in worsening of longitudinal involvement, whereas other components may remain preserved, thereby preserving EF. Whereas transmural dysfunction leads to loss of myocardial mechanics in all directions, resulting into LV dilation and reduction of LVEF.

SPECIFIC CLINICAL SCENARIOS

SUBCLINICAL MYOCARDIAL DYSFUNCTION. The longstanding presence of cardiovascular risk factors such as hypertension, diabetes mellitus, and obesity may cause disruption in the myocardial interstitial matrix as a result of microvascular ischemia, intramyocardial fibrosis, or collagen degradation product accumulation, leading to microscopic structural changes of the myofiber (18–20). These changes usually result in subclinical myocardial dysfunction at the endocardial level that can be detected using strain imaging as described earlier (reduction in GLS with compensatory increase in GCS and LVT with deterioration of diastolic function) (13). It is to be noted that similar changes also occur during the early subclinical stages and mild cases of infiltrative cardiac diseases. Because GLS is more reproducible and less variable than other parameters are and has proven clinical value, it is probably the single most important variable that can be used to identify and follow-up these patients.

Summary: Long-standing risk factors cause microscopic changes at the cellular level that affect the endocardial layer leading to depressed GLS and GRS, whereas GCS and LVT are relatively preserved due to the spared epicardial layer. GLS is of particular value in identifying and monitoring serial changes in these patients.

CORONARY ARTERY DISEASE. In patients with coronary artery disease (CAD), STE imaging has been applied extensively to reduce interobserver variability, to provide absolute cutoff values, and to assess "functional" transmurality of an infarction. Whereas visual assessments of regional systolic function, such as wall motion score index, are accepted methods of assessing myocardial ischemia and coronary heart disease, both at rest and during stress testing, these methods are greatly variable between readers and are expertise-demanding. On the other hand, 2D-STE strain imaging offers a relatively more robust and simpler method of assessing global and regional functions in patients with coronary heart disease at rest and during stress testing, allowing for less variability in the assessment of hypokinetic and dyskinetic segments (21).

Given the predominantly subendocardial involvement in ischemia, reduction of global and segmental GLS is an early abnormality seen in patients with CAD (**Figures 1A and 1C**). Reduced GLS can be used to diagnose CAD and the location of myocardial infarction (22), whereas augmentation of GLS during dobutamine stress echocardiography indicates global myocardial viability (**Figures 1B and 1D**). Segmental assessment of longitudinal strain (LS) is superior to visual assessment in identifying viable myocardial segments during low-dose dobutamine echocardiography (23), can be used to identify ischemic territories (24) and segments with ischemia-related post-systolic shortening (25,26), and to estimate infarct size.

Numerous studies have suggested clinical utility of regional strain in CAD (**Table 3**); however, improvement in the precision of regional strain will be required for making this technique clinically useful.

Summary: GLS can be effectively used in CAD and myocardial infarction for identifying ischemic territories and infarct size, respectively. Improvement of GLS and segmental LS values with dobutamine infusion is suggestive of global and segmental viability. Scarred and ischemic segments are associated with a reduction in other deformation parameters. Circumferential strain and LVT is preserved in subendocardial ischemia and is reduced in patients with transmural ischemia and infarction.

CARDIOMYOPATHIES. Dilated cardiomyopathy. Dilated cardiomyopathy (DCM) can be idiopathic or secondary to a variety of causes including ischemic heart disease, alcohol consumption, peripartum, chemotherapy, ventricular noncompaction, sarcoidosis, hemochromatosis, and myocarditis. The significant transmural myocardial remodeling that occurs in these patients is usually accompanied by loss of myocardial mechanics in all directions in parallel to the severity of LV systolic dysfunction. Both STE and FT-CMR studies have shown that the depressed GLS in these patients is of particular prognostic value and can be used to assess response to therapy and predict the occurrence of major cardiovascular events (27).

In addition to the abnormal strain values in patients with DCM, the increased sphericity of the LV apex affects the overall rotational mechanics and is usually accompanied by significant decrease in apical rotation and overall LVT. LV rotational mechanics, in addition to GLS, are other potential predictors of the response to cardiac resynchronization

FIGURE 1 STE in a Patient With Ischemic Cardiomyopathy During Low-Dose Dobutamine Viability Study

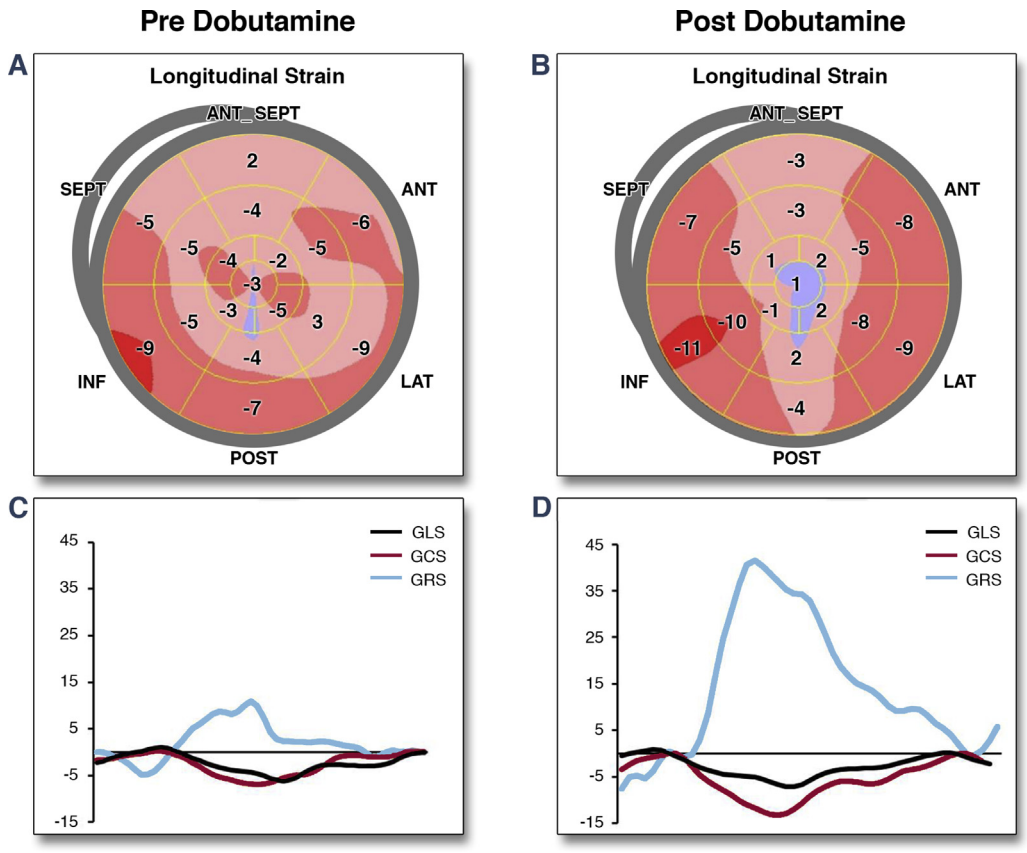

Polar maps at baseline **(A)** and peak dobutamine dose **(B)**. Strain curves at baseline **(C)** and peak dobutamine dose **(D)**. **(A,B)** Compared with baseline, segmental strain variables after dobutamine increased in the basal lateral and basal and mid anterior wall segments as well the basal posterior septum and basal and mid inferior wall segments, which is suggestive of viability. Moreover, strain in all directions (GLS, GCS, and GRS) increased at peak dobutamine compared with their baseline values, which is also suggestive of viability. ANT = anterior; GCS = global circumferential strain; GLS = global longitudinal strain; GRS = global radial strain; INF = inferior; LAT = lateral; POST = posterior; SEPT = septal; STE = speckle tracking echocardiography.

therapy (CRT) and rejection after transplantation (28,29).

Using FT-CMR, it was found that GLS is an independent predictor of survival in DCM and has incremental information for risk stratification beyond clinical parameters, biomarker, and standard CMR (30). STE-based studies found that strain can be a sensitive tool in early detection of cardiotoxicity especially in cancer patients being treated with chemotherapy. In female breast cancer patients treated with anthracyclines, GLS in combination with ultrasensitive troponin I was found to be predictive of the occurrence of chemotherapy-induced cardiotoxicity after 15 months of the completion of anthracyclines (31). GLS was also an independent predictor of LVEF in female breast cancer patients treated with trastuzumab (32). A recent systematic review found that early reduction of GLS by 10% to 15% is the most useful parameter in prediction of cardiotoxicity in patients receiving cancer chemotherapy (33).

In patients requiring CRT, an increase in GLS after implantation, in addition to the standard echocardiographic measurements, was found to predict responders and all-cause mortality at 1-year follow-up (34). A combined index of the magnitude and time of segmental radial strain was also found to be predictive of responders and survival 6 months post-implantation (35). Because of its ability to map temporal changes of strain distribution over the entire LV chamber, 3D-STE is considered a better modality for the analysis of LV dyssynchrony than 2D-STE is (36). Therefore, 3D-STE strain mapping may

TABLE 3 Tissue Tracking Technology in CAD

First Author, Year (Ref. #)	Patient Subgroup	Technology	Major Finding
Vitarelli et al., 2013 (62)	Chronic stable angina	2D-STE	GLS is better predictor of CAD severity than exercise ECG is
Sarvari et al., 2013 (90)	Non-STEMI	2D-STE	Subendocardial layer-specific strain is more depressed with significant CAD
Ersbøll et al., 2013 (91)	STEMI with preserved EF	2D-STE	GLS is better predictor of events than traditional risk factors are
Haugaa et al., 2010 (92) Ersbøll et al., 2013 (93)	Acute STEMI	2D-STE	Mechanical dispersion is predictive of sudden cardiac death or sustained VT
Shimoni et al., 2011 (94)	Coronary artery disease	2D-STE	All components of strain and strain rate are reduced and delayed in ischemic and scarred segments
Omar et al., 2015 (21)	ICM normal EF	2D-STE	LVT is preserved with subendocardial ischemia and reduced with transmural ischemia
Park et al., 2012 (95)	Acute STEMI	2D-STE	Apical rotation and LVT are reduced. LVT predicts functional recovery after 6 months
Seo et al., 2009 (96)	ICM	3D-STE	3D-STE confirms the extent of myocardial ischemia. Larger validation studies are lacking
Schneeweis et al., 2014 (97)	ICM	FT-CMR	FT-CMR improves diagnostic accuracy during dobutamine stress CMR
Schuster et al., 2011 (98)	ICM	FT-CMR	FT-CMR-derived parameters during low-dose dobutamine quantify the detection of myocardial viability and transmurality of infarction
Maret et al., 2009 (99)	Post-STEMI	FT-CMR	Radial strain is more predictive for scar transmurality than longitudinal endocardial strain is

2D = 2-dimensional; 3D = 3-dimensional; CAD = coronary artery disease; ECG = electrocardiography; EF = ejection fraction; ICM = ischemic cardiomyopathy; LVT = left ventricular twist; STE = speckle tracking echocardiography; STEMI = ST-segment elevation myocardial infarction; VT = ventricular tachycardia; other abbreviations as in Table 2.

be promising in prediction and assessment of response after CRT, but more studies and developments are needed.

Summary: DCM is associated with a significant decrease of myocardial deformation in all directions. GLS is of particular clinical value being able to monitor response to therapy, predict future events, and response to CRT.

Hypertrophic cardiomyopathy. Both fibrosis and hypertrophy contribute to abnormal myocardial mechanics in patients with hypertrophic cardiomyopathy (HCM). The increased wall stress and the relative endocardial ischemia together with the fibrotic changes lead to endocardial dysfunction and thus a prominent decrease in GLS (**Central Illustration**). Therefore, GLS can be effectively used to differentiate pathological hypertrophy from physiological hypertrophy that occurs in conditioned hearts of trained athletes, who show normal GLS values. Longitudinal septal strain, in particular, was found to be inversely related to the fibrotic changes in histopathology and to be a more powerful predictor of arrhythmia than late gadolinium enhancement is (37). GLS was also shown to predict adverse events in adults with HCM (38). The endocardial dysfunction noticed in HCM leads to depression of GRS; however, because of the epicardial layer thickening, these patients usually have increased LVT with delayed LV untwist (39). In 1 report (40), surgical myomectomy was found to normalize GCS and LVT in these patients.

Using FT-CMR, it was reported that patients with HCM have reduced longitudinal, radial, and circumferential strains compared with control subjects with the ability of radial and longitudinal strain to predict clinical outcome (41). Similar to STE studies, FT-CMR-derived LVT was found to be increased in patients with HCM, whereas LV untwist was delayed. In addition, peak LVT was significantly and independently related to the percentage of LV late gadolinium enhancement as well as myocardial thickness (42).

Summary: In patients with HCM, endocardial dysfunction causes decreased GLS and GRS, whereas the epicardial thickening leads to preserved GCS and LVT. GLS can be used to predict future response and, more importantly, to differentiate LV hypertrophy in HCM from that in athletes' hearts.

Restrictive cardiomyopathy. Restrictive cardiomyopathy (RCM) is caused by several infiltrative and storage diseases such as amyloidosis, sarcoidosis, systemic sclerosis, fibroelastosis, hemochromatosis, endomyocardial fibrosis, and eosinophilic endomyocardial disease (43). The microscopic deposition of these materials results in increased myocardial stiffness, which causes impaired ventricular filling with normal or decreased diastolic volume of either or both. Wall thickness may be normal or increased depending on the underlying cause.

Whatever the cause of RCM, GLS is always decreased. Myocardial GRS and GCS in RCM

FIGURE 2 Use of STE Parameters to Differentiate Between RCM and CP

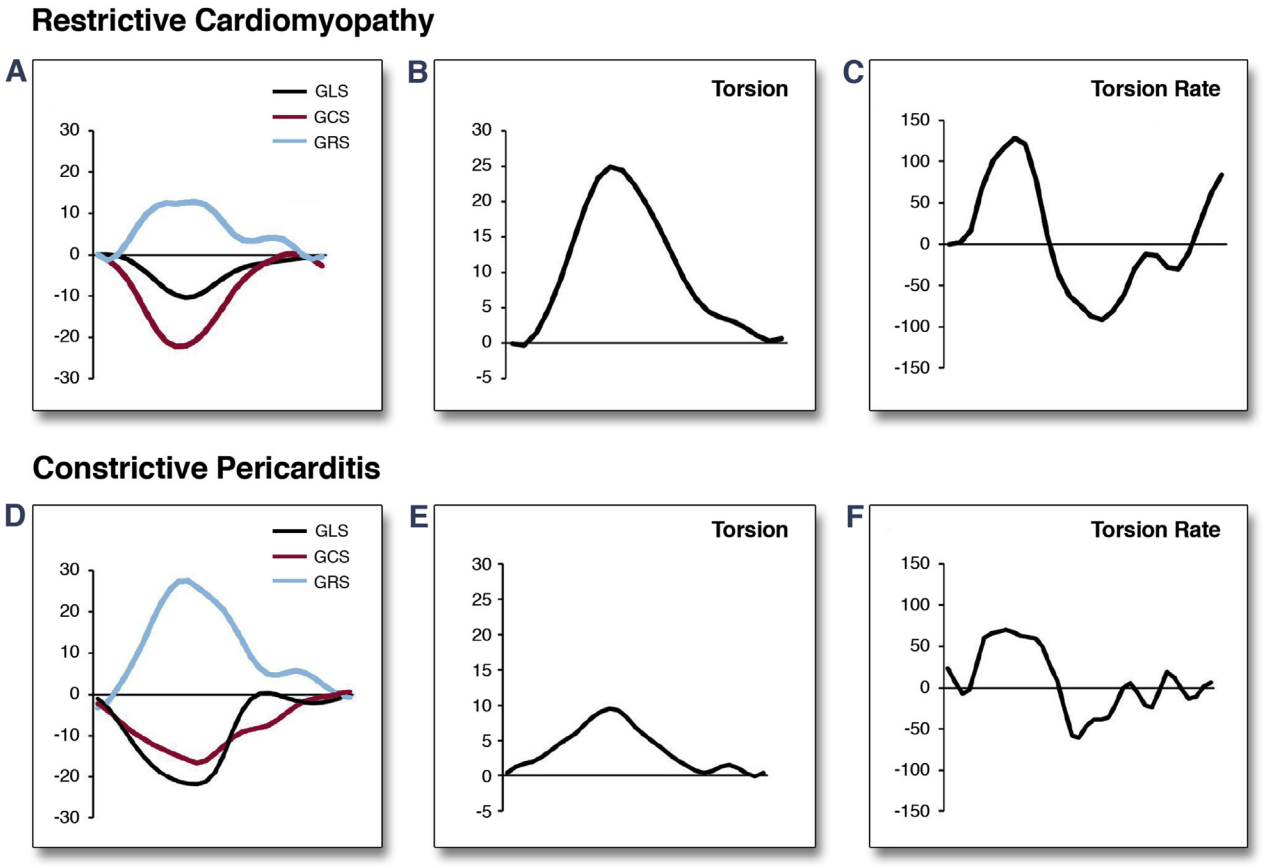

(A to C) In restrictive cardiomyopathy (RCM), the subendocardial fiber dysfunction will be associated with depressed GLS and GRS, whereas the spared epicardial fibers will lead to normal or increased GCS, left ventricular (LV) torsion, and LV torsional rate. **(D to F)** In constrictive pericarditis (CP), GLS and GRS are normal due to the spared endocardial fibers, whereas the affected epicardial fibers will be associated with depressed GCS, LV torsion, and LV torsional rate. Abbreviations as in Figure 1.

may remain compensated (44), and if impaired (45), will be related to the extent of cardiac involvement (46).

The most investigated cause of RCM is amyloidosis. Overall, GLS is decreased in amyloid heart disease as expected in a case of RCM and was found to be a negative predictor of survival (47). However, GLS in cardiac amyloidosis has a characteristic pattern with reduced strain at the LV base and progressively increased strain near the LV apex. LV twisting and untwisting motions are initially increased in patients with light-chain amyloidosis or systemic amyloidosis with no cardiac involvement (48,49), but they may normalize or become reduced with ongoing cardiac involvement (48). This may be helpful in differentiating amyloid-associated cardiac hypertrophy from HCM (46).

In patients with endomyocardial fibrosis (Fabry disease), in addition to the lower GLS (50), diastolic strain rates are also reduced (51,52), which correlated with the late gadolinium enhanced CMR (50). In patients with sarcoidosis and systemic sclerosis (53), GLS is also significantly reduced, and LVT might be slightly increased (54), and radial strain variations can differentiate sarcoidosis patients from those with DCM (55).

Summary: In patients with RCM, GLS is depressed significantly, whereas GRS and GCS might be preserved. In amyloid heart disease, beside the depressed GLS, LV twist and untwist might be preserved early and progressively decrease with the progression of cardiac involvement.

CONSTRICTIVE PERICARDITIS. Constrictive pericarditis (CP) is a pericardial disease with a particular

FIGURE 3 STE Parameters in a Patient With HFpEF Due to Long-Standing Hypertension

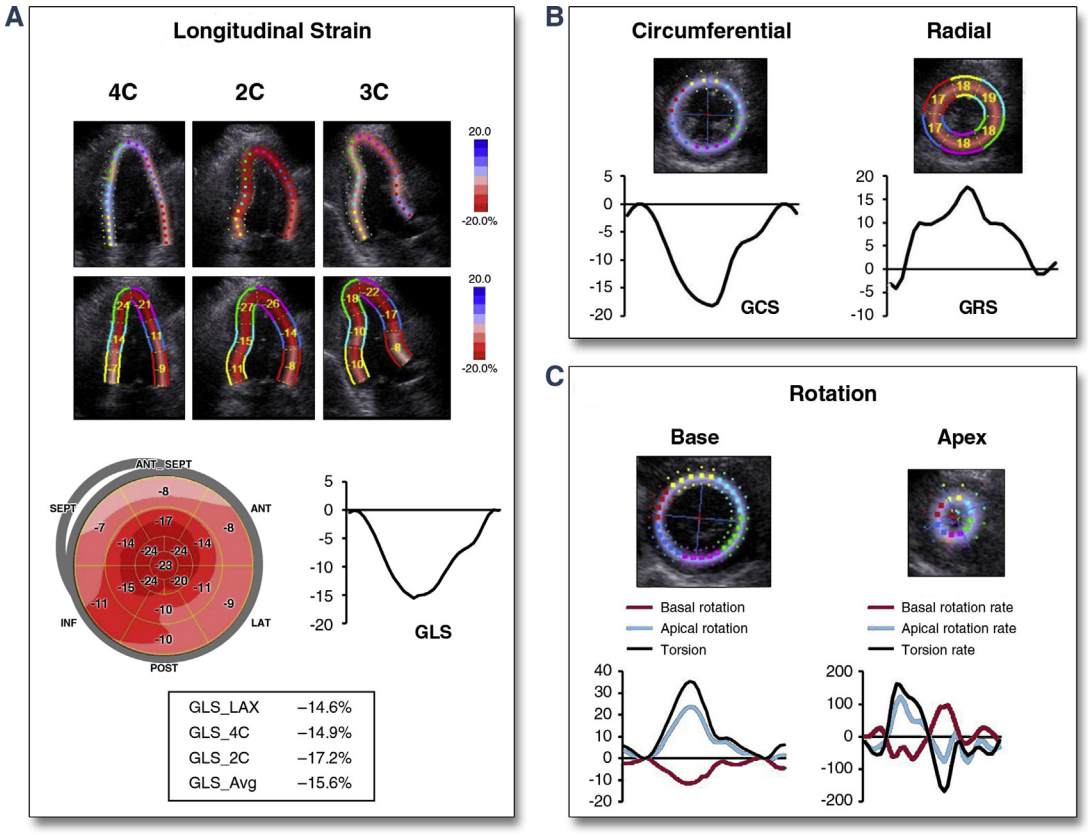

Endocardial border tracking for assessment of **(A)** GLS from the 3 apical views and **(B)** GCS and GRS from the short axis. **(C)** Endocardial border tracking in the short axis at the level of the LV base and apex for assessment of LV rotation and torsion. Although GLS and GRS are depressed, they are compensated by the relatively normal or increased GCS and LV torsion and thus the preserved ejection fraction. HFpEF = heart failure with preserved ejection fraction; LAX = measured on the long axis; other abbreviations as in Figures 1 and 2.

clinical importance, because its clinical picture can be mistaken for RCM, as both involve diastolic dysfunction with different mechanisms. Thus differentiation between both conditions is challenging using the conventional methods. STE-derived deformation imaging can usually give a clue to differentiate both conditions, as different myocardial layers are affected and thus each case exhibits different mechanical behaviors. In RCM, endocardial dysfunction causes depression in GLS and GRS. The relatively spared epicardial fibers cause preservation of GCS and LVT (Figures 2A to 2C). In contrast, in CP, mainly the subepicardial fibers are affected with relative sparing of subendocardial fibers, which leads to preserved GLS and GRS, whereas GCS and LVT are usually depressed (Figures 2D to 2F) (44).

Summary: Deformation imaging can be used to assess patients with pericardial diseases and to differentiate CP from RCM. In CP, the epicardial dysfunction leads to depressed GCS and LVT, whereas GLS and GRS are preserved, compared with RCM where the endocardial dysfunction causes depression of GLS and GRS with preserved GCS and LVT.

VALVULAR HEART DISEASE. In patients with aortic stenosis (AS) and preserved EF, the subendocardial ischemia resulting from the pressure-overload causes attenuation of GLS with relative preservation or increase in LVT (56). Treatment of AS by surgical or transcatheter aortic valve replacement cause normalization of all LV mechanics (56,57).

FT-CMR was used to compare the impact of a transfemoral to a transapical approach of transcatheter aortic valve replacement on myocardial mechanics (58). No differences in peak radial or longitudinal strain were found for the basal and mid-segments. Not surprisingly, in the transapical

approach peak radial and longitudinal strain were reduced with respect to the transfemoral approach in the apical segments and the apical cap.

In patients with mitral regurgitation (MR) and normal EF, the development of insidious myocardial dysfunction is usually associated with depression in GLS, GCS, and GRS (59), whereas LVT might be preserved until the development of evident reduction of EF (60). In MR patients undergoing mitral valve repair, pre-procedural GLS was found to predict post-procedural EF reduction (61). In patients with secondary significant MR undergoing mitral clip, 3D-STE showed overall improvement in both LV and RV strain after clip implantation (62).

In patients with mitral stenosis, GLS and GCS were found to be lower than in control subjects, with continuous normalization within 72 h after balloon mitral valvuloplasty (63). In addition, LVT was found to be lower in patients with mitral stenosis (64). It is still controversial whether the basal decrease in LV mechanics in patients with mitral stenosis is due to LV dysfunction or as a result of decreased pre-load caused by the stenosed valve.

Summary: In AS, endocardial dysfunction leads to depressed GLS, whereas LVT is usually preserved. All deformation parameters tend to normalize after valve replacement. In MR, depression of strain parameters is a sign of insidious systolic dysfunction. GLS can predict post-mitral valve repair EF reduction.

MYOCARDIAL MECHANICS IN HEART FAILURE. Systolic heart failure. Symptoms of heart failure can develop despite preserved EF (i.e., heart failure with preserved ejection fraction [HFpEF]). It was previously believed that the main pathophysiological changes only involve abnormal diastolic function; however, LV strain studies have shown that concomitant systolic abnormalities do occur (15,65). Ongoing progression of the underlying pathology may result in abnormalities in strain in all directions resulting into heart failure with reduced ejection fraction (HFrEF).

STE-based studies have shown that a decreased GLS can be used as a marker of insidious systolic function in HFpEF patients and is associated with higher levels of pro-B-type natriuretic peptide levels and worse diastolic function (**Figure 3A**) (66). Exercise is usually associated with further depression of GLS and provocation of symptoms in these patients. The development of abnormal endocardial function early in the course of heart failure is responsible for the abnormal longitudinal function. The reason why EF is preserved in these patients is that GCS and LVT remain unchanged or even increased (**Figures 3B and 3C**), compensating for the decreased GLS. With the development of HFrEF, GLS continues to decrease together with failure of the compensating mechanisms of LVT and GCS, thus myocardial pump failure and dilation usually ensue (**Figure 4**).

Summary: In HFpEF, endocardial dysfunction leads to depressed GLS, which correlates with levels of pro-B-type natriuretic peptide and diastolic functions. The preserved GCS and LVT usually compensates for the depressed GLS. Failure of these compensatory mechanisms later in the course of the disease lead to pump failure (HFrEF).

Diastolic dysfunction and assessment of filling pressures. Deformation imaging provides unique information during the diastolic period that can potentially be useful in the assessment of diastolic function. This includes the quantification of segmental and global diastolic strain rate, as well as the differences in the timing of transition from myocardial contraction to relaxation with strain rate imaging (67). Whereas most of these parameters were used in the assessment of regional fibrosis and ischemia, a few studies have shown a significant relation between segmental and global early diastolic strain rate and the time constant of LV relaxation (tau) (68,69).

LV diastolic untwist contributes to early LV filling through the generation of negative suction pressure (21). Untwisting parameters were shown to correlate with invasive indices of LV relaxation and suction (first derivative of pressure measured over time [dP/dt] and tau) but not with LV stiffness, suggesting that untwisting is a key mechanical event that aids LV early diastolic filling because of serving as a link between systolic compression and early diastolic recoil (21,67). Importantly, in cases with abnormal LV relaxation, untwist duration and time to peak untwist rate are directly related to tau (21).

However, untwist rate, in addition to LV relaxation, is also affected by systolic contraction and thus, changes in untwist rate might not be an accurate representation of the diastolic dysfunction in patients with HFpEF.

Although there are plenty of studies concerned with the assessment of diastolic functions using STE, there is relatively less data available for the use of CMR in the assessment of LV diastolic function. Nevertheless, studies have employed myocardial tagging to demonstrate abnormalities in LV untwisting in diastole in conditions such as asymptomatic individuals with LV hypertrophy and AS (70). In the MESA (Multi-Ethnic Study of Atherosclerosis), CMR tagging was found to be useful in the assessment of regional diastolic function non-invasively. In those patients, regional impairment of early diastolic strain rate was found to occur despite the preserved systolic function (70,71). Moreover, in

FIGURE 4 STE Parameters in a Patient With HFrEF Due to Long-Standing Hypertension

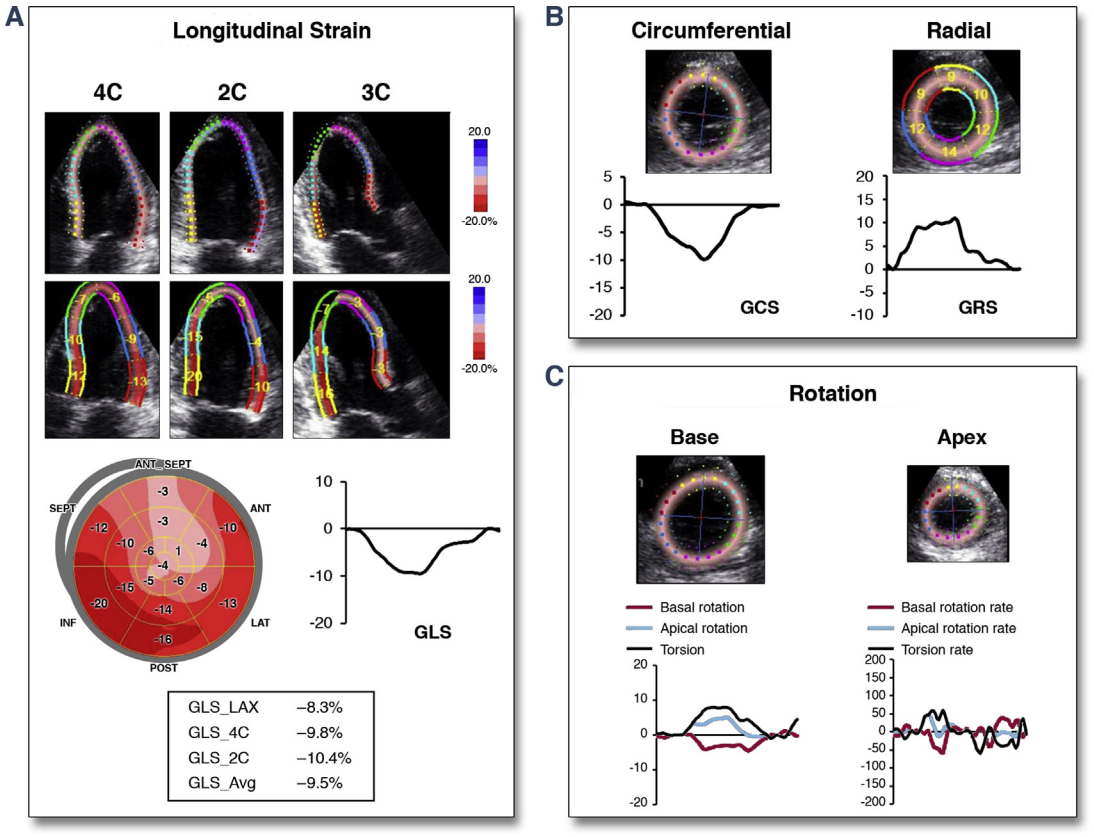

Endocardial border tracking for assessment of **(A)** GLS from the 3 apical views and **(B)** GCS and GRS from the short axis. **(C)** Endocardial border tracking in the short axis at the level of LV base and apex for assessment of LV rotation and torsion. All strain values (GLS, GRS, and GCS) as well as LV torsion are significantly depressed, signifying exhaustion of compensation mechanisms. HFrEF = heart failure with reduced ejection fraction; other abbreviations as in Figures 1 to 3.

a subset of patients in the CARDIA (Coronary Artery Risk Development in Young Adults) study, diastolic strain rate calculated from tagged magnetic resonance images was found to predict incident heart failure and atrial fibrillation (72).

Summary: Tissue tracking parameters can be used to assess LV relaxation and diastolic function. LV untwist and strain rate might be promising in this regard. In patients with diastolic dysfunction, prolonged and delayed LV untwist is particularly related to prolonged LV relaxation and tau and worse LV diastolic suction.

CLINICAL USE OF DEFORMATION IMAGING IN OTHER CARDIAC CHAMBERS

RIGHT VENTRICULAR FUNCTION. The use of RV-LS derived from the RV free wall is currently recommended for the assessment of RV functions in patients with suspected RV dysfunctions, such as congenital abnormalities, arrhythmogenic RV cardiomyopathy, pulmonary, primary arterial hypertension (PAH), and pulmonary thromboembolism. In those patients, RV-LS values are usually decreased and delayed (73). Interventions that cause improvement of hemodynamics in these patients are usually accompanied by improvement in RV-LS.

In general, RV function derived from STE was shown to have prognostic value in a variety of congenital abnormalities (74-76). In patients with tetralogy of Fallot, RV-LS correlated with exercise capacity (76).

However, LV affection in patients with RV dysfunction, as a manifestation of ventricular interdependence, is not uncommon. For instance, in patients with PAH, LV septal circumferential strain was found to be affected more than the RV free wall LS was (77). Moreover, RV strain was found to

correlate with LV filling pressure, and combination of both parameters as a measure of interdependence might serve as a predictor for future outcome in patients with PAH (78).

In patients with arrhythmogenic right ventricular cardiomyopathy (ARVC), compared with control subjects, RV-LS derived from either STE or FT-CMR was found to be significantly depressed (10,79) and to be superior to conventional echocardiographic parameters when used for the diagnosis of these patients.

It was also found that in patients with ARVC, compared with control subjects, RV-LS fails to increase with exercise (62). Furthermore, 2D-STE have suggested a high incidence of LV involvement in phenotypic patients with ARVC as well as genetically predisposed relatives. LV involvement in addition to an enlarged RV outflow tract were found to be independent prognostic markers of event-free survival (80).

Summary: RV-LS is a recommended measure to assess RV function in clinical scenarios with suspected RV dysfunction. RV dysfunction caused by PAH, congenital anomalies, and ARVC is usually associated by depressed RV-LS. RV-LS is also of prognostic value in these patients.

Left atrial function. STE and FT-CMR can be also used to assess LA longitudinal deformations. Because the LA is a thin-walled chamber, the measurement of the radial deformation is difficult. LA strain and strain rate can be used to study LA conduit, contractile, and reservoir functions (81) and are considered promising tools that can be used for the assessment of LV filling pressures (81,82). In patients with HCM and HFpEF, FT-CMR–derived total strain and positive strain rates were reduced and both LA conduit function strain during ventricular E-wave and first negative strain rate were impaired (12).

In a substudy of MESA, patients had lower atrial GLS and higher indexed minimal LA volume, both of which were independently associated with incident heart failure, even after adjusting for traditional risk factors, LV mass and N-terminal pro-B-type natriuretic peptide (70). FT-CMR–derived LA LS and strain rate were also found to reliably discriminate between patients with impaired LV relaxation and healthy control subjects (12).

LA strain measures, however, are not currently recommended for routine clinical use and remain mainly promising research tools, primarily because most studies concerned with their use are small.

Summary: LA-LS can be assessed by tissue tracking and is a promising tool that can be used for assessment of LV filling pressures and atrial function; however, it still remains as a research tool awaiting clinical validation.

FUTURE RESEARCH DIRECTIONS

SPECKLE TRACKING ECHOCARDIOGRAPHY. Variability in most of the STE-derived parameters remains a great concern and creates difficulties in standardizing their use and application in everyday clinical practice (5). The recently initiated European Society of Cardiovascular Imaging and the American Society of Echocardiography strain standardization task force is aiming at addressing the issue of variability by standardizing the use and applications of STE between different vendors' software and users (4).

Importantly, because 3D-STE can simultaneously measure myocardial motion in all directions, the introduction of high-resolution 3D systems can be used for the assessment of myocardial principal strain, a newly developed concept of studying myocardial mechanics using 3D echocardiography, which simultaneously integrates myocardial deformations in all directions, alleviating the need for multidirectional strain assessments (83). In the future, limitations in the spatial-temporal resolution may be addressed with the incorporation of high-frequency ultrasound systems, which represent a new frontier for echocardiographic-based deformation imaging that promises high temporal and spatial resolutions (84).

Finally, appreciation of the LV intracavitary vortex motion and studying its interaction with myocardial deformations may open a new era of exploring the mechanical efficiency of cardiac contractions (85).

CMR FEATURE TRACKING. As opposed to speckle tracking, FT-CMR has not been validated in the setting of phantoms or animal models to compare with ground truth assessment of myocardial deformation by, for example, crystals.

In many pathologies, early subclinical changes are detected by changes of LS. However, because GLS and especially global RV-LS are less reproducible than GCS is, optimization of the longitudinal tracking will be necessary to be applicable in the individual patient. The major advantage of FT-CMR is that it does not require special sequences and can be applied retrospectively. Therefore, it can be expected that this technique will see a large increase in published studies, as was the case after the introduction of STE replacing the tissue Doppler-based strain imaging techniques.

As opposed to STE (6), most FT-CMR studies have been using the same software for analysis, limiting this potential source of variability. It can be

TABLE 4 Patterns of Myocardial Deformation in Different Cardiovascular Diseases

	GLS	GRS	GCS	LVT	LV-UTR
Cardiac risk factor–induced subclinical myocardial dysfunction	↓	↓	Normal or↑	Normal or ↑	Normal or ↓
Ischemic heart disease	↓	↓	Normal or ↑	Normal or ↑	Delayed/may ↓
Dilated cardiomyopathy	↓	↓	↓	↓	↓
LV noncompaction	↓	↓	↓	Absent	Absent
Hypertrophic cardiomyopathy	↓	↓	Normal or ↑	Normal or ↑	Delayed/may ↓
Restrictive cardiomyopathy	↓	↓	↓	↓	↓
Constrictive pericarditis	Normal	Normal	↓	↓	↓
Aortic stenosis	↓	↓	Normal or ↑	Normal or ↑	Delayed/may ↓
Mitral regurgitation	↓	↓	Normal or ↑	Normal or ↑	Delayed/may ↓
Heart failure preserved ejection fraction	↓	↓	Normal or ↑	Normal or ↑	Normal or ↓
Heart failure reduced ejection fraction	↓	↓	↓	↓	↓

↓ = decrease; ↑ = increase; UTR = untwist rate; other abbreviations as in Tables 2 and 3.

expected that when FT-CMR enters more into the clinical arena, new software will emerge and similar efforts of standardization like with STE will be needed (4).

There is a large transmural gradient (from endocardium to epicardium) of circumferential strain and a slightly different initial contour placement will influence circumferential strain values. The optimal choice here remains unknown and will need to be determined by further research or consensus. In this context, it is also important to remember that FT-CMR derives its information mainly from the endocardial border, as opposed to intramyocardial speckles as used for STE.

FT-CMR offers the possibility to use historical cine data. Although the effect of frame rate has not been studied, so far the standard frame rate used in CMR (usually approximately 30 frames/cardiac cycle) is below the recommended frame rates for STE, which may induce significant differences especially when considering strain rate values.

CONCLUSIONS

Both STE and FT-CMR currently offer reproducible measurements of global strain values that can be applied in different clinical scenarios to assess LV and RV function (Table 4). CMR has an established and continuously expanding role in tissue characterization and is the modality of choice for accurate evaluation of global function using volumetry. Whether the additional assessment of myocardial deformation yields information beyond direct tissue characterization remains to be evaluated. Similarly, the yield of STE versus CMR tissue characterization needs to be assessed. Most likely, a major clinical value of these techniques will only be achieved when a reliable segmental analysis becomes possible. For the time being, GLS in 2D-STE has a proven clinical value due to its sensitivity to early contractile changes in the presence of normal or preserved EF.

REPRINT REQUESTS AND CORRESPONDENCE: Prof. Eike Nagel, Institute of Experimental and Translational Cardiovascular Imaging, DZHK Centre for Cardiovascular Imaging Interdisciplinary Cardiovascular Imaging, Internal Medicine III and Institute for Diagnostic and Interventional Radiology, University Hospital Frankfurt-Main, Frankfurt, Germany. E-mail: eike.nagel@cardiac-imaging.org.

REFERENCES

1. Bohs LN, Trahey GE. A novel method for angle independent ultrasonic imaging of blood flow and tissue motion. IEEE Trans Biomed Eng 1991;38:280–6.

2. Kaluzynski K, Chen X, Emelianov SY, Skovoroda AR, O'Donnell M. Strain rate imaging using two-dimensional speckle tracking. IEEE Trans Ultrason Ferroelectr Freq Control 2001;48:1111–23.

3. Hor KN, Gottliebson WM, Carson C, et al. Comparison of magnetic resonance feature tracking for strain calculation with harmonic phase imaging analysis. J Am Coll Cardiol Img 2010;3:144–51.

4. Voigt JU, Pedrizzetti G, Lysyansky P, et al. Definitions for a common standard for 2D speckle tracking echocardiography: consensus document of the EACVI/ASE/Industry Task Force to standardize deformation imaging. Eur Heart J Cardiovasc Imaging 2015;16:1–11.

5. Mor-Avi V, Lang RM, Badano LP, et al. Current and evolving echocardiographic techniques for the quantitative evaluation of cardiac mechanics: ASE/EAE consensus statement on methodology and indications endorsed by the Japanese Society of Echocardiography. J Am Soc Echocardiogr 2011;24:277–313.

6. Lang RM, Badano LP, Mor-Avi V, et al. Recommendations for cardiac chamber quantification by echocardiography in adults: an update from the American Society of Echocardiography and the European Association of

Cardiovascular Imaging. J Am Soc Echocardiogr 2015;28:1–39.e14.

7. Nagata Y, Takeuchi M, Mizukoshi K, et al. Intervendor variability of two-dimensional strain using vendor-specific and vendor-independent software. J Am Soc Echocardiogr 2015;28:630–41.

8. Yingchoncharoen T, Agarwal S, Popović ZB, Marwick TH. Normal ranges of left ventricular strain: a meta-analysis. J Am Soc Echocardiogr 2013;26:185–91.

9. Schuster A, Morton G, Hussain ST, et al. The intra-observer reproducibility of cardiovascular magnetic resonance myocardial feature tracking strain assessment is independent of field strength. Eur J Radiol 2013;82:296–301.

10. Heermann P, Hedderich DM, Paul M, et al. Biventricular myocardial strain analysis in patients with arrhythmogenic right ventricular cardiomyopathy (ARVC) using cardiovascular magnetic resonance feature tracking. J Cardiovasc Magn Reson 2014;16:75.

11. Evin M, Cluzel P, Lamy J, et al. Assessment of left atrial function by MRI myocardial feature tracking. J Magn Reson Imaging 2015;42:379–89.

12. Kowallick J, Kutty S, Edelmann F, et al. Quantification of left atrial strain and strain rate using Cardiovascular Magnetic Resonance myocardial feature tracking: a feasibility study. J Cardiovasc Magn Reson 2014;16:60.

13. Sengupta PP, Narula J. Reclassifying heart failure: predominantly subendocardial, subepicardial, and transmural. Heart Fail Clin 2008;4:379–82.

14. Sengupta PP, Tajik AJ, Chandrasekaran K, Khandheria BK. Twist mechanics of the left ventricle: principles and application. J Am Coll Cardiol Img 2008;1:366–76.

15. Vinereanu D, Lim PO, Frenneaux MP, Fraser AG. Reduced myocardial velocities of left ventricular long-axis contraction identify both systolic and diastolic heart failure—a comparison with brain natriuretic peptide. Eur J Heart Fail 2005;7:512–9.

16. Zhang J. Myocardial energetics in cardiac hypertrophy. Clin Exp Pharmacol Physiol 2002;29:351–9.

17. Tea BS, Dam TV, Moreau P, Hamet P, deBlois D. Apoptosis during regression of cardiac hypertrophy in spontaneously hypertensive rats: temporal regulation and spatial heterogeneity. Hypertension 1999;34:229–35.

18. Crendal E, Walther G, Vinet A, et al. Myocardial deformation and twist mechanics in adults with metabolic syndrome: impact of cumulative metabolic burden. Obesity (Silver Spring) 2013;21:E679–86.

19. Jellis C, Martin J, Narula J, Marwick TH. Assessment of nonischemic myocardial fibrosis. J Am Coll Cardiol 2010;56:89–97.

20. Maharaj N, Khandheria BK, Libhaber E, et al. Relationship between left ventricular twist and circulating biomarkers of collagen turnover in hypertensive patients with heart failure. J Am Soc Echocardiogr 2014;27:1064–71.

21. Omar AM, Vallabhajosyula S, Sengupta PP. Left ventricular twist and torsion: research observations and clinical applications. Circ Cardiovasc Imaging 2015;8:pii:e003029.

22. Montgomery DE, Puthumana JJ, Fox JM, Ogunyankin KO. Global longitudinal strain aids the detection of non-obstructive coronary artery disease in the resting echocardiogram. Eur Heart J Cardiovasc Imaging 2012;13:579–87.

23. Ng AC, Sitges M, Pham PN, et al. Incremental value of 2-dimensional speckle tracking strain imaging to wall motion analysis for detection of coronary artery disease in patients undergoing dobutamine stress echocardiography. Am Heart J 2009;158:836–44.

24. Dandel M, Hetzer R. Echocardiographic strain and strain rate imaging—clinical applications. Int J Cardiol 2009;132:11–24.

25. Asanuma T, Uranishi A, Masuda K, Ishikura F, Beppu S, Nakatani S. Assessment of myocardial ischemic memory using persistence of post-systolic thickening after recovery from ischemia. J Am Coll Cardiol Img 2009;2:1253–61.

26. Asanuma T, Fukuta Y, Masuda K, Hioki A, Iwasaki M, Nakatani S. Assessment of myocardial ischemic memory using speckle tracking echocardiography. J Am Coll Cardiol Img 2012;5:1–11.

27. Nahum J, Bensaid A, Dussault C, et al. Impact of longitudinal myocardial deformation on the prognosis of chronic heart failure patients. Circ Cardiovasc Imaging 2010;3:249–56.

28. Clemmensen TS, Løgstrup BB, Eiskjaer H, Poulsen SH. Changes in longitudinal myocardial deformation during acute cardiac rejection: the clinical role of two-dimensional speckle-tracking echocardiography. J Am Soc Echocardiogr 2015;28:330–9.

29. Bernard A, Donal E, Leclercq C, et al. Impact of cardiac resynchronization therapy on left ventricular mechanics: understanding the response through a new quantitative approach based on longitudinal strain integrals. J Am Soc Echocardiogr 2015;28:700–8.

30. Buss SJ, Breuninger K, Lehrke S, et al. Assessment of myocardial deformation with cardiac magnetic resonance strain imaging improves risk stratification in patients with dilated cardiomyopathy. Eur Heart J Cardiovasc Imaging 2015;16:307–15.

31. Sawaya H, Sebag IA, Plana JC, et al. Assessment of echocardiography and biomarkers for the extended prediction of cardiotoxicity in patients treated with anthracyclines, taxanes, and trastuzumab. Circ Cardiovasc Imaging 2012;5:596–603.

32. Negishi K, Negishi T, Haluska BA, Hare JL, Plana JC, Marwick TH. Use of speckle strain to assess left ventricular responses to cardiotoxic chemotherapy and cardioprotection. Eur Heart J Cardiovasc Imaging 2014;15:324–31.

33. Thavendiranathan P, Poulin F, Lim KD, Plana JC, Woo A, Marwick TH. Use of myocardial strain imaging by echocardiography for the early detection of cardiotoxicity in patients during and after cancer chemotherapy: a systematic review. J Am Coll Cardiol 2014;63:2751–68.

34. Park HC, Shin J, Ban JE, Choi JI, Park SW, Kim YH. Left atrial appendage: morphology and function in patients with paroxysmal and persistent atrial fibrillation. Int J Cardiovasc Imaging 2013;29:935–44.

35. Kydd AC, Khan FZ, O'Halloran D, Pugh PJ, Virdee MS, Dutka DP. Radial strain delay based on segmental timing and strain amplitude predicts left ventricular reverse remodeling and survival after cardiac resynchronization therapy. Circ Cardiovasc Imaging 2013;6:177–84.

36. Tanaka H, Hara H, Saba S, Gorcsan J 3rd. Usefulness of three-dimensional speckle tracking strain to quantify dyssynchrony and the site of latest mechanical activation. Am J Cardiol 2010;105:235–42.

37. Almaas VM, Haugaa KH, Strøm EH, et al. Noninvasive assessment of myocardial fibrosis in patients with obstructive hypertrophic cardiomyopathy. Heart 2014;100:631–8.

38. Reant P, Reynaud A, Pillois X, et al. Comparison of resting and exercise echocardiographic parameters as indicators of outcomes in hypertrophic cardiomyopathy. J Am Soc Echocardiogr 2015;28:194–203.

39. Geyer H, Caracciolo G, Abe H, et al. Assessment of myocardial mechanics using speckle tracking echocardiography: fundamentals and clinical applications. J Am Soc Echocardiogr 2010;23:351–69.

40. Moravsky G, Bruchal-Garbicz B, Jamorski M, et al. Myocardial mechanical remodeling after septal myectomy for severe obstructive hypertrophic cardiomyopathy. J Am Soc Echocardiogr 2013;26:893–900.

41. Smith BM, Dorfman AL, Yu S, et al. Relation of strain by feature tracking and clinical outcome in children, adolescents, and young adults with hypertrophic cardiomyopathy. Am J Cardiol 2014;114:1275–80.

42. Nucifora G, Muser D, Morocutti G, et al. Disease-specific differences of left ventricular rotational mechanics between cardiac amyloidosis and hypertrophic cardiomyopathy. Am J Physiol Heart Circ Physiol 2014;307:H680–8.

43. Hancock EW. Differential diagnosis of restrictive cardiomyopathy and constrictive pericarditis. Heart 2001;86:343–9.

44. Sengupta PP, Krishnamoorthy VK, Abhayaratna WP, et al. Disparate patterns of left ventricular mechanics differentiate constrictive pericarditis from restrictive cardiomyopathy. J Am Coll Cardiol Img 2008;1:29–38.

45. Di Bella G, Minutoli F, Pingitore A, et al. Endocardial and epicardial deformations in cardiac amyloidosis and hypertrophic cardiomyopathy. Circ J 2011;75:1200–8.

46. Baccouche H, Maunz M, Beck T, et al. Differentiating cardiac amyloidosis and hypertrophic cardiomyopathy by use of three-dimensional speckle tracking echocardiography. Echocardiography 2012;29:668–77.

47. Quarta CC, Solomon SD, Uraizee I, et al. Left ventricular structure and function in transthyretin-related versus light-chain cardiac amyloidosis. Circulation 2014;129:1840–9.

48. Cappelli F, Porciani MC, Bergesio F, et al. Characteristics of left ventricular rotational mechanics in patients with systemic amyloidosis,

systemic hypertension and normal left ventricular mass. Clin Physiol Funct Imaging 2011;31:159–65.

49. Porciani MC, Cappelli F, Perfetto F, et al. Rotational mechanics of the left ventricle in AL amyloidosis. Echocardiography 2010;27:1061–8.

50. Krämer J, Niemann M, Liu D, et al. Two-dimensional speckle tracking as a non-invasive tool for identification of myocardial fibrosis in Fabry disease. Eur Heart J 2013;34:1587–96.

51. Shanks M, Thompson RB, Paterson ID, et al. Systolic and diastolic function assessment in Fabry disease patients using speckle-tracking imaging and comparison with conventional echocardiographic measurements. J Am Soc Echocardiogr 2013;26:1407–14.

52. Saccheri MC, Cianciulli TF, Lax JA, et al., for the AADELFA Investigators. Two-dimensional speckle tracking echocardiography for early detection of myocardial damage in young patients with Fabry disease. Echocardiography 2013;30:1069–77.

53. Spethmann S, Dreger H, Schattke S, et al. Two-dimensional speckle tracking of the left ventricle in patients with systemic sclerosis for an early detection of myocardial involvement. Eur Heart J Cardiovasc Imaging 2012;13:863–70.

54. Aggeli C, Felekos I, Tousoulis D, Gialafos E, Rapti A, Stefanadis C. Myocardial mechanics for the early detection of cardiac sarcoidosis. Int J Cardiol 2013;168:4820–1.

55. Tsuji T, Tanaka H, Matsumoto K, et al. Capability of three-dimensional speckle tracking radial strain for identification of patients with cardiac sarcoidosis. Int J Cardiovasc Imaging 2013;29:317–24.

56. Carasso S, Cohen O, Mutlak D, et al. Relation of myocardial mechanics in severe aortic stenosis to left ventricular ejection fraction and response to aortic valve replacement. Am J Cardiol 2011;107:1052–7.

57. Poulin F, Carasso S, Horlick EM, et al. Recovery of left ventricular mechanics after transcatheter aortic valve implantation: effects of baseline ventricular function and postprocedural aortic regurgitation. J Am Soc Echocardiogr 2014;27:1133–42.

58. Meyer CG, Frick M, Lotfi S, et al. Regional left ventricular function after transapical vs. transfemoral transcatheter aortic valve implantation analysed by cardiac magnetic resonance feature tracking. Eur Heart J Cardiovasc Imaging 2014;15:1168–76.

59. Kim MS, Kim YJ, Kim HK, et al. Evaluation of left ventricular short- and long-axis function in severe mitral regurgitation using 2-dimensional strain echocardiography. Am Heart J 2009;157:345–51.

60. Zito C, Carerj S, Todaro MC, et al. Myocardial deformation and rotational profiles in mitral valve prolapse. Am J Cardiol 2013;112:984–90.

61. Pandis D, Sengupta PP, Castillo JG, et al. Assessment of longitudinal myocardial mechanics in patients with degenerative mitral valve regurgitation predicts postoperative worsening of left ventricular systolic function. J Am Soc Echocardiogr 2014;27:627–38.

62. Vitarelli A, Cortes Morichetti M, Capotosto L, et al. Utility of strain echocardiography at rest and after stress testing in arrhythmogenic right ventricular dysplasia. Am J Cardiol 2013;111:1344–50.

63. Sengupta SP, Amaki M, Bansal M, et al. Effects of percutaneous balloon mitral valvuloplasty on left ventricular deformation in patients with isolated severe mitral stenosis: a speckle-tracking strain echocardiographic study. J Am Soc Echocardiogr 2014;27:639–47.

64. Kirilmaz B, Asgun F, Saygi S, Ercan E. Decreased left ventricular torsion in patients with isolated mitral stenosis. Herz 2015;40:123–8.

65. Yu CM, Lin H, Yang H, Kong SL, Zhang Q, Lee SW. Progression of systolic abnormalities in patients with "isolated" diastolic heart failure and diastolic dysfunction. Circulation 2002;105:1195–201.

66. Kraigher-Krainer E, Shah AM, Gupta DK, et al., for the PARAMOUNT Investigators. Impaired systolic function by strain imaging in heart failure with preserved ejection fraction. J Am Coll Cardiol 2014;63:447–56.

67. Nagueh SF, Appleton CP, Gillebert TC, et al. Recommendations for the evaluation of left ventricular diastolic function by echocardiography. J Am Soc Echocardiogr 2009;22:107–33.

68. Kato T, Noda A, Izawa H, et al. Myocardial velocity gradient as a noninvasively determined index of left ventricular diastolic dysfunction in patients with hypertrophic cardiomyopathy. J Am Coll Cardiol 2003;42:278–85.

69. Wang J, Khoury DS, Thohan V, Torre-Amione G, Nagueh SF. Global diastolic strain rate for the assessment of left ventricular relaxation and filling pressures. Circulation 2007;115:1376–83.

70. Habibi M, Chahal H, Opdahl A, et al. Association of CMR-measured LA function with heart failure development: results from the MESA study. J Am Coll Cardiol Img 2014;7:570–9.

71. Edvardsen T, Rosen BD, Pan L, et al. Regional diastolic dysfunction in individuals with left ventricular hypertrophy measured by tagged magnetic resonance imaging—the Multi-Ethnic Study of Atherosclerosis (MESA). Am Heart J 2006;151:109–14.

72. Ambale-Venkatesh B, Armstrong AC, Liu CY, et al. Diastolic function assessed from tagged MRI predicts heart failure and atrial fibrillation over an 8-year follow-up period: the Multi-Ethnic Study of Atherosclerosis. Eur Heart J Cardiovasc Imaging 2014;15:442–9.

73. Pirat B, McCulloch ML, Zoghbi WA. Evaluation of global and regional right ventricular systolic function in patients with pulmonary hypertension using a novel speckle tracking method. Am J Cardiol 2006;98:699–704.

74. Heiberg J, Ringgaard S, Schmidt MR, Redington A, Hjortdal VE. Structural and functional alterations of the right ventricle are common in adults operated for ventricular septal defect as toddlers. Eur Heart J Cardiovasc Imaging 2015;16:483–9.

75. Schmidt R, Orwat S, Kempny A, et al. Value of speckle-tracking echocardiography and MRI-based feature tracking analysis in adult patients after Fontan-type palliation. Congenit Heart Dis 2014;9:397–406.

76. Kempny A, Fernández-Jiménez R, Orwat S, et al. Quantification of biventricular myocardial function using cardiac magnetic resonance feature tracking, endocardial border delineation and echocardiographic speckle tracking in patients with repaired tetralogy of Fallot and healthy controls. J Cardiovasc Magn Reson 2012;14:32.

77. Querejeta Roca G, Campbell P, Claggett B, et al. Impact of lowering pulmonary vascular resistance on right and left ventricular deformation in pulmonary arterial hypertension. Eur J Heart Fail 2015;17:63–73.

78. Motoji Y, Tanaka H, Fukuda Y, et al. Interdependence of right ventricular systolic function and left ventricular filling and its association with outcome for patients with pulmonary hypertension. Int J Cardiovasc Imaging 2015;31:691–8.

79. Teske AJ, Cox MG, De Boeck BW, Doevendans PA, Hauer RN, Cramer MJ. Echocardiographic tissue deformation imaging quantifies abnormal regional right ventricular function in arrhythmogenic right ventricular dysplasia/cardiomyopathy. J Am Soc Echocardiogr 2009;22:920–7.

80. Mast TP, Teske AJ, Vd Heijden JF, et al. Left ventricular involvement in arrhythmogenic right ventricular dysplasia/cardiomyopathy assessed by echocardiography predicts adverse clinical outcome. J Am Soc Echocardiogr 2015;28:1103–13.e9.

81. Saraiva RM, Demirkol S, Buakhamsri A, et al. Left atrial strain measured by two-dimensional speckle tracking represents a new tool to evaluate left atrial function. J Am Soc Echocardiogr 2010;23:172–80.

82. Kurt M, Tanboga IH, Aksakal E, et al. Relation of left ventricular end-diastolic pressure and N-terminal pro-brain natriuretic peptide level with left atrial deformation parameters. Eur Heart J Cardiovasc Imaging 2012;13:524–30.

83. Pedrizzetti G, Sengupta S, Caracciolo G, et al. Three-dimensional principal strain analysis for characterizing subclinical changes in left ventricular function. J Am Soc Echocardiogr 2014;27:1041–50.e1.

84. Bhan A, Sirker A, Zhang J, et al. High-frequency speckle tracking echocardiography in the assessment of left ventricular function and remodeling after murine myocardial infarction. Am J Physiol Heart Circ Physiol 2014;306:H1371–83.

85. Abe H, Caracciolo G, Kheradvar A, et al. Contrast echocardiography for assessing left ventricular vortex strength in heart failure: a prospective cohort study. Eur Heart J Cardiovasc Imaging 2013;14:1049–60.

86. Augustine D, Lewandowski AJ, Lazdam M, et al. Global and regional left ventricular myocardial deformation measures by magnetic resonance feature tracking in healthy volunteers: comparison with tagging and relevance of gender. J Cardiovasc Magn Reson 2013;15:8.

87. Morton G, Schuster A, Jogiya R, Kutty S, Beerbaum P, Nagel E. Inter-study reproducibility of cardiovascular magnetic resonance myocardial

feature tracking. J Cardiovasc Magn Reson 2012; 14:43.

88. Kutty S, Rangamani S, Venkataraman J, et al. Reduced global longitudinal and radial strain with normal left ventricular ejection fraction late after effective repair of aortic coarctation: a CMR feature tracking study. Int J Cardiovasc Imaging 2013;29:141–50.

89. Padiyath A, Gribben P, Abraham JR, et al. Echocardiography and cardiac magnetic resonance-based feature tracking in the assessment of myocardial mechanics in tetralogy of Fallot: an intermodality comparison. Echocardiography 2013; 30:203–10.

90. Sarvari SI, Haugaa KH, Zahid W, et al. Layer-specific quantification of myocardial deformation by strain echocardiography may reveal significant CAD in patients with non-ST-segment elevation acute coronary syndrome. J Am Coll Cardiol Img 2013;6:535–44.

91. Ersbøll M, Valeur N, Mogensen UM, et al. Prediction of all-cause mortality and heart failure admissions from global left ventricular longitudinal strain in patients with acute myocardial infarction and preserved left ventricular ejection fraction. J Am Coll Cardiol 2013;61:2365–73.

92. Haugaa KH, Smedsrud MK, Steen T, et al. Mechanical dispersion assessed by myocardial strain in patients after myocardial infarction for risk prediction of ventricular arrhythmia. J Am Coll Cardiol Img 2010;3:247–56.

93. Ersbøll M, Valeur N, Andersen MJ, et al. Early echocardiographic deformation analysis for the prediction of sudden cardiac death and life-threatening arrhythmias after myocardial infarction. J Am Coll Cardiol Img 2013;6:851–60.

94. Shimoni S, Gendelman G, Ayzenberg O, et al. Differential effects of coronary artery stenosis on myocardial function: the value of myocardial strain analysis for the detection of coronary artery disease. J Am Soc Echocardiogr 2011;24:748–57.

95. Park SM, Hong SJ, Ahn CM, et al. Different impacts of acute myocardial infarction on left ventricular apical and basal rotation. Eur Heart J Cardiovasc Imaging 2012;13:483–9.

96. Seo Y, Ishizu T, Enomoto Y, et al. Validation of 3-dimensional speckle tracking imaging to quantify regional myocardial deformation. Circ Cardiovasc Imaging 2009;2:451–9.

97. Schneeweis C, Qiu J, Schnackenburg B, et al. Value of additional strain analysis with feature tracking in dobutamine stress cardiovascular magnetic resonance for detecting coronary artery disease. J Cardiovasc Magn Reson 2014;16:72.

98. Schuster A, Kutty S, Padiyath A, et al. Cardiovascular magnetic resonance myocardial feature tracking detects quantitative wall motion during dobutamine stress. J Cardiovasc Magn Reson 2011; 13:58.

99. Maret E, Todt T, Brudin L, et al. Functional measurements based on feature tracking of cine magnetic resonance images identify left ventricular segments with myocardial scar. Cardiovasc Ultrasound 2009;7:53.

KEY WORDS cardiac mechanics, feature-tracking cardiac magnetic resonance imaging, myocardial function, speckle tracking echocardiography

APPENDIX For the supplemental material, please see the online version of this article.